

# Experimental Determination of Phase Equilibria in the Ag-Cu-Sb Ternary System

X.J. Liu, X.F. Yang, S.Y. Yang, and C.P. Wang

(Submitted May 16, 2015; in revised form August 11, 2015; published online September 24, 2015)

Phase equilibria of the Ag-Cu-Sb system were experimentally determined by electron probe microanalyzer and x-ray diffraction. Three isothermal sections of the Ag-Cu-Sb ternary system at 300, 500 and 600 °C were experimentally established, and no ternary compound was found in this system. Experimental results show that the liquid phase region increases with the temperature increase in region from 500 to 600 °C. The newly determined phase equilibria in this system will provide important information for the development of lead-free solders.

**Keywords** Ag-Cu-Sb, metals and alloys, phase diagram, x-ray diffraction

## 1. Introduction

In many available solder alloys, the lead-tin alloys have been the most commonly used in electronic interconnection and packaging so far, because of their low cost and good combination of physical, chemical, mechanical properties, manufacturability and reliability. However, in consideration of environmental and health concerns, substantial researches are currently being carried out to develop alternative solder alloys that may be capable of substitution for traditionally used lead bearing solder alloys.<sup>[1]</sup> For a variety of reasons, the most prominent lead-free solder alloys are likely to be tin-based alloys, with alloying elements such as Cu, Sb, Ag, Zn and Bi, etc. In order to design such lead-free substitute solder alloys, various phases equilibria of candidate systems are necessary.

The family of Sn-Ag lead-free solders are considered as the most promising candidate to replace the conventional lead-tin solder alloy so far, and there are many experimental and thermodynamic studies for the Sn-Ag, Sn-Ag-Cu<sup>[2]</sup> and Sn-Ag-Sb<sup>[3]</sup> lead-free solders systems. As lead-free solders Sn-Ag, Sn-Ag-Cu and Sn-Ag-Sb systems, each has its own superior characteristics as well as some drawbacks. Most recently, a new solder with small amount of Sb in Sn-Ag-Cu system has been regarded as the most promising candidate for the replacement of Sn-Pb solders, because it has better mechanical properties of strength, elongation, creep and fatigue resistance than Sn-Ag solders. However, the optimal

amount of Sb has not been reported, it is necessary to investigate the sub-ternary systems of the Sn-Ag-Cu-Sb quaternary database, which can further help us explore the optimal amount of Sb. As sub-ternary systems of the quaternary Sn-Ag-Cu-Sb system, the experimental and thermodynamic information of Sn-Ag-Cu,<sup>[2]</sup> Sn-Ag-Sb,<sup>[3]</sup> and Sn-Cu-Sb<sup>[4]</sup> ternary systems are available. It is of great importance to exert an experiment for the Ag-Cu-Sb ternary systems which can further help us explore the solder alloys possessing great properties. Based on the experimental investigations and thermodynamic calculations, the present authors have developed the thermodynamic database of lead-free solder,<sup>[5–9]</sup> but the phase equilibria of the Ag-Cu-Sb systems is still missing. Therefore the purpose of our present work is to experimentally investigate the phase equilibria of the Ag-Cu-Sb system at the temperatures of 300, 500 and 600 °C, by electron probe microanalyzer (EPMA) and x-ray diffraction (XRD).

Three binary systems Ag-Cu,<sup>[10]</sup> Ag-Sb,<sup>[11]</sup> Cu-Sb,<sup>[12]</sup> constituting the Ag-Cu-Sb ternary system, are shown in Fig. 1. Some researchers have investigated the phase diagram of the Ag-Cu binary system.<sup>[10,13–15]</sup> It has been reported that the Ag-Cu binary system is a simple system without any intermediate phase. The Ag-Sb binary phase diagram assessed by Okamoto et al. was adopted in this work due to the good agreement with the experimental data.<sup>[16]</sup> The Ag-Sb binary system has two intermediate phases, namely  $\zeta$  (Ag<sub>7</sub>Sb) and  $\epsilon$  (Ag<sub>3</sub>Sb). The  $\zeta$  (Ag<sub>7</sub>Sb) phase is formed through the peritectic reaction:  $L + (\text{Ag}) \leftrightarrow \zeta (\text{Ag}_7\text{Sb})$  at 702.5 °C, and  $\epsilon$  (Ag<sub>3</sub>Sb) phase is formed through peritectic reaction:  $L + \zeta (\text{Ag}_7\text{Sb}) \leftrightarrow \epsilon (\text{Ag}_3\text{Sb})$  at 558 °C. The phase diagram of the Cu-Sb binary system was studied by many researchers.<sup>[12,17–20]</sup> These previous investigations show that the Cu-Sb binary system has six intermediate phases,  $\epsilon$  (Cu, Sb),  $\eta$  (Cu<sub>2</sub>Sb),  $\beta$  (Cu, Sb),  $\zeta$  (Cu, Sb),  $\delta$  (Cu, Sb) and  $\gamma$  (Cu, Sb). The  $\beta$  (Cu, Sb) phase is formed through monotectic transition:  $L \leftrightarrow L + \beta (\text{Cu, Sb})$  at 683 °C. The  $\delta$  (Cu, Sb) and  $\zeta$  (Cu, Sb) phases were demonstrated to be the results of these reactions:  $\gamma (\text{Cu, Sb}) + \beta (\text{Cu, Sb}) \leftrightarrow \delta (\text{Cu, Sb})$ ,  $\delta (\text{Cu, Sb}) + \epsilon (\text{Cu, Sb}) \leftrightarrow \zeta (\text{Cu, Sb})$ . The information of the stable solid phases in the three binary systems is summarized in Table 1.

X.J. Liu, S.Y. Yang, and C.P. Wang, Department of Materials Science and Engineering, College of Materials, Xiamen, 361005, P.R. China and Research Center of Materials Design and Applications, Xiamen University, Xiamen, 361005, P.R. China; and X.F. Yang, Department of Materials Science and Engineering, College of Materials, Xiamen 361005, P.R. China. Contact e-mail: wangcp@xmu.edu.cn.

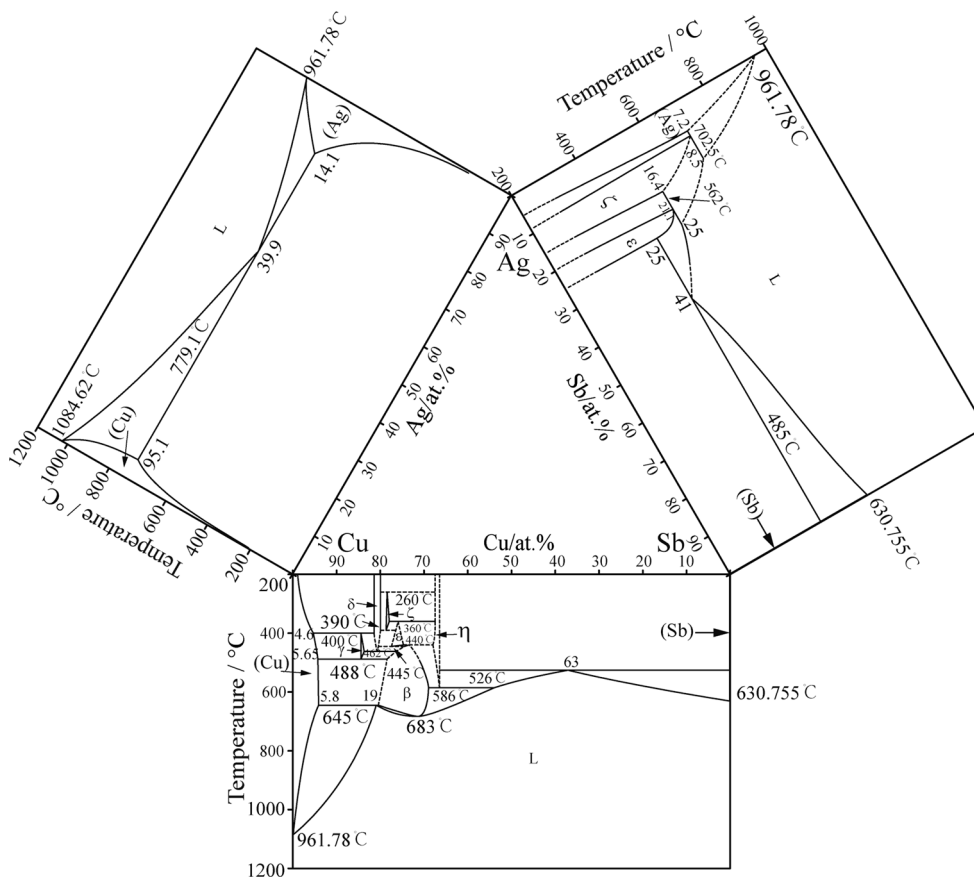


Fig. 1 Binary phase diagrams constituting the Ag-Cu-Sb ternary system<sup>[10–12]</sup>

Table 1 The stable solid phases in the three binary systems<sup>[10–12]</sup>

System	Phase	Pearson's symbol	Space group	Prototype	Strukturbericht designation	References
Ag-Cu	(Ag)	<i>cF4</i>	<i>Fm-3m</i>	Cu	A1	[10]
	(Cu)	<i>cF4</i>	<i>Fm-3m</i>	Cu	A1	[10]
Ag-Sb	(Ag)	<i>cF4</i>	<i>Fm-3m</i>	Cu	A1	[11]
	ζ	<i>hp2</i>	<i>P6<sub>3</sub>/mmc</i>	Mg	A3	[11]
	ε-Ag <sub>3</sub> Sb	<i>tp4</i>	<i>P4/mmm</i>	Cu <sub>3</sub> Ti	L6 <sub>0</sub>	[11]
	(Sb)	<i>hR2</i>	<i>R-3m</i>	As	A7	[11]
Cu-Sb	(Cu)	<i>cF4</i>	<i>Fm-3m</i>	Cu	A1	[12]
	β	<i>cF16</i>	<i>Fm-3m</i>	BiF <sub>3</sub>	D0 <sub>3</sub>	[12]
	γ	<i>hP2</i>	<i>P6<sub>3</sub>/mmc</i>	Mg	A3	[12]
	δ	<i>Hp*</i>	<i>P6<sub>3</sub>/mmc</i>	...	...	[12]
	ε	<i>oP8</i>	<i>Pmmn</i>	βCu <sub>3</sub> Ti	D0 <sub>a</sub>	[12]
	ζ	<i>hp26</i>	<i>P-3</i>	Cu <sub>10</sub> Sb <sub>3</sub>	...	[12]
	η	<i>tp6</i>	<i>P4/mmm</i>	Cu <sub>2</sub> Sb	C38	[12]
	(Sb)	<i>hR2</i>	<i>R-3m</i>	αAs	A7	[12]

## 2. Experimental Procedure

Copper (99.9 wt.%), Silver (99.9 wt.%), Antimony (99.9 wt.%) were used as starting materials. The elements were weighted with an accuracy of 0.001 g and sealed in quartz capsules in an argon atmosphere against oxidation.

Each sample was heated at 800 °C and remained at this temperature for 1 days, followed by quenching in water using a bottom-quenching technique to minimize the loss of Sb. It is a special quenching technique in order to minimize the development of porosity in the samples during cooling. It was found that by immersing only the bottom half of the

quartz tube in the cooling water, so that the surface of the liquid alloy was kept above the water level, a relatively compact sample could be obtained. In this way, a temperature gradient was established along the length of the quartz tube which favoured the condensation of Sb vapour in the space above the liquid back onto the liquid, and discouraged the evaporation of the liquid.<sup>[21]</sup> The weight of sample was around 20 g, and the weight of loss during melting was generally less than 0.2%. Afterwards, the samples were cut into small pieces for heat treatments. The specimens were annealed at 300, 500 and 600 °C, respectively. The time of heat treatment varied from 2 h to 2 months depending on the annealing temperature. After the heat treatment, the specimens were quenched into iced water.

After annealing and standard metallographic preparation, optical microscope (OM) was used to confirm the metallographic preparation was fine and then the microstructure images of specimens were carried out by back-scattered electron (BSE). The equilibrium compositions of the phases were measured by EPMA (JXA-8100R, JEOL, Japan). The measurements were carried out at a voltage of 20.0 kV with the standard of pure elements. Microprobe measurements for each equilibrium phase was taken on seven points to get high accuracy. The composition of the liquid phase was determined via area analysis using EDS at 20.0 kV. Seven area measurements on liquid phase were made to decrease the statistical error. At the same time, the maximum and minimum values were removed, and the final values were the average of remaining. The constituent phases of the alloys were further determined by analyzing XRD patterns generated by a Phillips PANalytical X-pert diffractometer, operating at 40.0 kV and 30 mA with Cu K $\alpha$  radiation. The data were collected in the range of  $2\theta$  from 20° to 80° at a step of 0.0167°.

### 3. Results and Discussion

#### 3.1 Microstructure and Phase Equilibria

BSE images of typical ternary Ag-Cu-Sb alloys annealed at 300, 500 and 600 °C are presented in Fig. 2. Phase identification was based on the equilibrium composition measured by EPMA (Table 2) and XRD results (Fig. 3).

The three-phase equilibrium of the A<sub>7</sub>(Sb) +  $\epsilon$  (Ag<sub>3</sub>Sb) +  $\eta$  (Cu<sub>2</sub>Sb) is identified in the Ag<sub>20</sub>Cu<sub>40</sub>Sb<sub>40</sub> (at.%) alloy annealed at 300 °C for 60 days, its microstructure is shown in Fig. 2(a). The crystal structure of its three-phase is identified by the XRD in Fig. 3(a), where in which characteristic peaks of the A<sub>7</sub>(Sb),  $\epsilon$  (Ag<sub>3</sub>Sb) and  $\eta$  (Cu<sub>2</sub>Sb) phase are marked by different symbols. Figure 2(b) shows the three-phase microstructure  $\eta$  (Cu<sub>2</sub>Sb) +  $\delta$  (Cu, Sb) +  $\zeta$  (Ag<sub>7</sub>Sb) of the Ag<sub>20</sub>Cu<sub>60</sub>Sb<sub>20</sub> (at.%) alloy annealed at 300 °C for 60 days. Its XRD result is shown in Fig. 3(b). Figure 2(c) presents the three-phase microstructure of the FCC(Cu) +  $\delta$  (Cu, Sb) +  $\zeta$  (Ag<sub>7</sub>Sb) in the Ag<sub>5</sub>Cu<sub>85</sub>Sb<sub>10</sub>

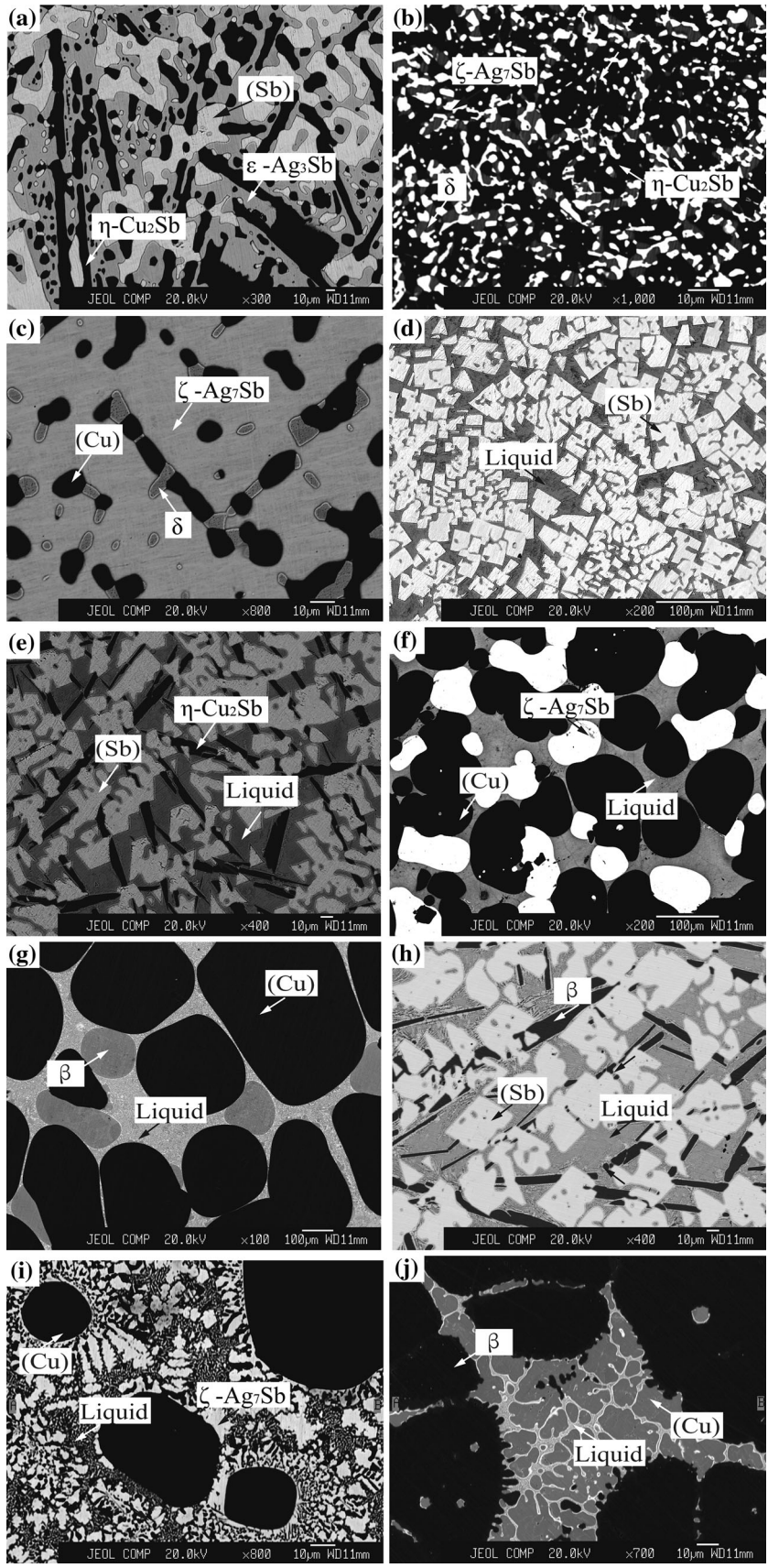
(at.%) alloy annealed at 300 °C for 60 days. Two-phase microstructure can be observed in the Ag<sub>20</sub>Cu<sub>10</sub>Sb<sub>70</sub> (at.%) alloy quenched from 500 °C for 2 days and the same alloy quenched from 600 °C for 2 h, as showed in Fig. 2(d). Figure 2(e) shows the typical BSE image of the three-phase microstructure of the Liquid + A<sub>7</sub>(Sb) +  $\eta$  (Cu<sub>2</sub>Sb) in the Ag<sub>20</sub>Cu<sub>20</sub>Sb<sub>60</sub> (at.%) alloy annealed at 500 °C for 2 days. The three-phase equilibrium of the Liquid + FCC (Cu) +  $\zeta$  (Ag<sub>7</sub>Sb) is identified in the Ag<sub>20</sub>Cu<sub>75</sub>Sb<sub>5</sub> (at.%) alloy annealed at 500 °C for 2 days, as indicated in Fig. 2(f). In the Ag<sub>5</sub>Cu<sub>85</sub>Sb<sub>10</sub> (at.%) alloy annealed at 500 °C for 2 days, a three-phase equilibrium Liquid + FCC (Cu) +  $\beta$  (Cu, Sb) is found, as shown in Fig. 2(g). Figure 2(h) presents the three phase microstructure of the Liquid +  $\beta$  (Cu, Sb) + A<sub>7</sub>(Sb) in the Ag<sub>20</sub>Cu<sub>20</sub>Sb<sub>60</sub> (at.%) alloy annealed at 600 °C for 2 h. Figure 2(i) shows the three-phase microstructure of the Liquid + FCC (Cu) +  $\zeta$  (Ag<sub>7</sub>Sb) in the Ag<sub>20</sub>Cu<sub>75</sub>Sb<sub>5</sub> (at.%) alloy and Fig. 2(j) shows the three-phase microstructure of the Liquid +  $\beta$  (Cu, Sb) + FCC (Cu) in the Ag<sub>5</sub>Cu<sub>85</sub>Sb<sub>10</sub> (at.%) alloy annealed at 600 °C for 2 h.

#### 3.2 Isothermal Sections

The equilibrium compositions of the Ag-Cu-Sb ternary system at 300, 500 and 600 °C determined by EPMA are summarized in Table 2. Based on the obtained experimental data mentioned above, the isothermal sections at 300, 500 and 600 °C have been constructed in Fig. 4. Undetermined three-phase equilibria are labeled in dashed lines.

In the isothermal section at 300 °C (Fig. 4a), three three-phase regions of the A<sub>7</sub>(Sb) +  $\epsilon$  (Ag<sub>3</sub>Sb) +  $\eta$  (Cu<sub>2</sub>Sb),  $\eta$  (Cu<sub>2</sub>Sb) +  $\delta$  (Cu, Sb) +  $\zeta$  (Ag<sub>7</sub>Sb) and FCC(Cu) +  $\delta$  (Ag, Sb) +  $\zeta$  (Ag<sub>7</sub>Sb) were experimentally determined in this work. The solubility of Ag and Cu in (Sb) is extremely low, and the solubility of Cu in the  $\epsilon$  (Ag<sub>3</sub>Sb) and  $\zeta$  (Ag<sub>7</sub>Sb) is about 2.6 and 2.5 at.% through the determined isothermal section. In addition, the solubility of Ag in  $\delta$  (Cu, Sb) is measured to be about 1.5 at.%, and the solubility of Ag in  $\eta$  (Cu<sub>2</sub>Sb) is about 1.2 at.%.

Figure 4(b) shows the isothermal section at 500 °C, where the three-phase equilibrium of the Liquid + A<sub>7</sub>(Sb) +  $\eta$  (Cu<sub>2</sub>Sb), Liquid + FCC (Cu) +  $\zeta$  (Ag<sub>7</sub>Sb) and Liquid +  $\beta$  (Cu, Sb) + FCC (Cu) were experimentally determined in this work. Three three-phase regions, the  $\zeta$  (Ag<sub>7</sub>Sb) +  $\epsilon$  (Ag<sub>3</sub>Sb) + Liquid, FCC (Cu) + FCC (Ag) +  $\zeta$  (Ag<sub>7</sub>Sb) and  $\eta$  (Cu<sub>2</sub>Sb) +  $\beta$  (Cu, Sb) + Liquid were not determined in this work because their regions are too small. In the isothermal section at 600 °C, shown in Fig. 4(c), three three-phase regions of the Liquid + A<sub>7</sub>(Sb) +  $\beta$  (Cu, Sb), Liquid + FCC (Cu) +  $\zeta$  (Ag<sub>7</sub>Sb) and Liquid +  $\beta$  (Cu, Sb) + FCC (Cu) were experimentally determined. Compared with the isothermal sections determined by the present work, it is clearly shown that there is a large area of liquid phase at 500 and 600 °C isothermal sections. In the present work, no ternary compound in this system was found. In the



◀ **Fig. 2** Typical ternary BSE images obtained from: (a) the Ag<sub>20</sub>Cu<sub>40</sub>Sb<sub>40</sub> (at.%) alloy annealed at 300 °C for 60 days; (b) the Ag<sub>20</sub>Cu<sub>60</sub>Sb<sub>20</sub> (at.%) alloy annealed at 300 °C for 60 days; (c) the Ag<sub>5</sub>Cu<sub>85</sub>Sb<sub>10</sub> (at.%) alloy annealed at 300 °C for 60 days; (d) the Ag<sub>20</sub>Cu<sub>10</sub>Sb<sub>70</sub> (at.%) alloy annealed at 500 °C for 2 days; (e) the Ag<sub>20</sub>Cu<sub>20</sub>Sb<sub>60</sub> (at.%) alloy annealed at 500 °C for 2 days; (f) the Ag<sub>20</sub>Cu<sub>75</sub>Sb<sub>5</sub> (at.%) alloy annealed at 500 °C for 2 days; (g) the Ag<sub>5</sub>Cu<sub>85</sub>Sb<sub>10</sub> (at.%) alloy annealed at 500 °C for 2 days; (h) the Ag<sub>20</sub>Cu<sub>20</sub>Sb<sub>60</sub> (at.%) alloy annealed at 600 °C for 2 h; (i) the Ag<sub>20</sub>Cu<sub>75</sub>Sb<sub>5</sub> (at.%) alloy annealed at 600 °C for 2 h; (j) the Ag<sub>5</sub>Cu<sub>85</sub>Sb<sub>10</sub> (at.%) alloy annealed at 600 °C for 2 h

light of the experiment results, the addition of Sb to the family of Sn-Ag lead-free solder must be less than 5 at.%, because excessive Sb may promote the formation of some brittle compounds, such as ε (Ag<sub>3</sub>Sb), ζ (Ag<sub>7</sub>Sb) and η (Cu<sub>2</sub>Sb), which may worsen the mechanical properties of the solder joints.

#### 4. Conclusions

The isothermal sections of the Ag-Cu-Sb system at 300, 500 and 600 °C are determined experimentally, and no ternary compound was found in this system. Experimental results show that the liquid phase region increases with the increase in temperature region from 500 to 600 °C. The phase equilibrium of the Ag-Cu-Sb ternary system determined in the present work will provide additional support for the thermodynamic assessment of this system and practical application for the lead-free solders.

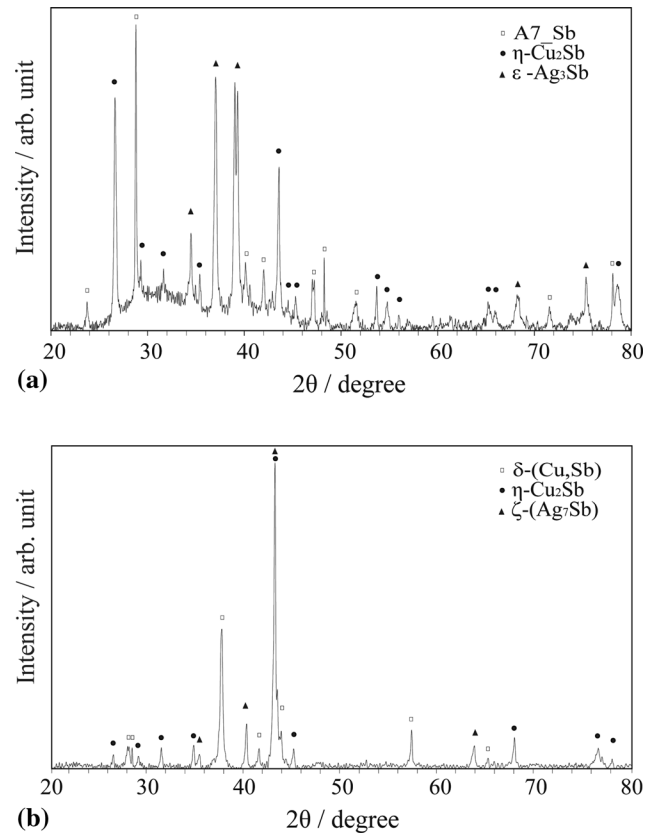


**Fig. 3** X-ray diffraction patterns obtained from: (a) the Ag<sub>20</sub>Cu<sub>40</sub>Sb<sub>40</sub> (at.%) alloy annealed at 300 °C for 60 days; (b) the Ag<sub>20</sub>Cu<sub>60</sub>Sb<sub>20</sub> (at.%) alloy annealed at 300 °C for 60 days

**Table 2** Equilibrium compositions of the Ag-Cu-Sb ternary system determined in the present work

Temperature, °C	Alloy, at.%	Annealed time	Phase equilibria	Composition, at.%					
				Phase 1		Phase 2		Phase 3	
				Sb	Ag	Sb	Ag	Sb	Ag
300	Ag <sub>20</sub> Cu <sub>10</sub> Sb <sub>70</sub>	60 days	Cu <sub>2</sub> Sb/Ag <sub>3</sub> Sb/(Sb)	33.34	1.14	23.56	75.14	99.1	0.84
	Ag <sub>20</sub> Cu <sub>20</sub> Sb <sub>60</sub>	60 days	Cu <sub>2</sub> Sb/Ag <sub>3</sub> Sb/(Sb)	34.12	1.06	22.95	75.15	98.9	1.02
	Ag <sub>20</sub> Cu <sub>40</sub> Sb <sub>40</sub>	60 days	Cu <sub>2</sub> Sb/Ag <sub>3</sub> Sb/(Sb)	33.89	1.16	23.22	75.21	99.3	0.65
	Ag <sub>20</sub> Cu <sub>60</sub> Sb <sub>20</sub>	60 days	Cu <sub>2</sub> Sb/δ/Ag <sub>7</sub> Sb	32.56	0.98	19.76	1.56	12.79	85.04
	Ag <sub>20</sub> Cu <sub>75</sub> Sb <sub>5</sub>	60 days	Cu/δ/Ag <sub>7</sub> Sb	3.79	1.05	18.91	1.46	10.78	86.75
	Ag <sub>5</sub> Cu <sub>85</sub> Sb <sub>10</sub>	60 days	Cu/δ/Ag <sub>7</sub> Sb	3.78	1.09	19.23	1.39	10.98	86.57
500	Ag <sub>20</sub> Cu <sub>10</sub> Sb <sub>70</sub>	2 days	Liquid/(Sb)	43.78	42.56	99.76	0.03		
	Ag <sub>20</sub> Cu <sub>20</sub> Sb <sub>60</sub>	2 days	Liquid/Cu <sub>2</sub> Sb/(Sb)	39.58	40.56	35.23	1.65	99.61	0.01
	Ag <sub>5</sub> Cu <sub>40</sub> Sb <sub>55</sub>	2 days	Liquid/Cu <sub>2</sub> Sb/(Sb)	38.81	41.27	34.02	1.83	99.50	0.06
	Ag <sub>20</sub> Cu <sub>75</sub> Sb <sub>5</sub>	2 days	Liquid/(Cu)/Ag <sub>7</sub> Sb	22.97	35.35	2.63	1.21	11.92	87.68
	Ag <sub>5</sub> Cu <sub>85</sub> Sb <sub>10</sub>	2 days	Liquid/(Cu)/β	22.38	29.16	2.84	1.02	22.50	3.16
600	Ag <sub>20</sub> Cu <sub>10</sub> Sb <sub>70</sub>	2 h	Liquid/(Sb)	46.37	32.56	99.59	0.11		
	Ag <sub>20</sub> Cu <sub>20</sub> Sb <sub>60</sub>	2 h	Liquid/β/(Sb)	36.45	33.16	32.64	2.93	99.03	0.14
	Ag <sub>5</sub> Cu <sub>40</sub> Sb <sub>55</sub>	2 h	Liquid/β/(Sb)	35.36	32.44	33.23	3.21	98.86	0.07
	Ag <sub>20</sub> Cu <sub>75</sub> Sb <sub>5</sub>	2 h	Liquid/Ag <sub>7</sub> Sb/(Cu)	17.87	32.16	10.17	87.72	2.45	2.34
	Ag <sub>5</sub> Cu <sub>85</sub> Sb <sub>10</sub>	2 h	Liquid/β/(Cu)	20.16	25.85	23.14	3.21	3.68	1.23

Five analyses were carried out for each phase and the standard deviation of the measured concentration is ±0.5 at.%

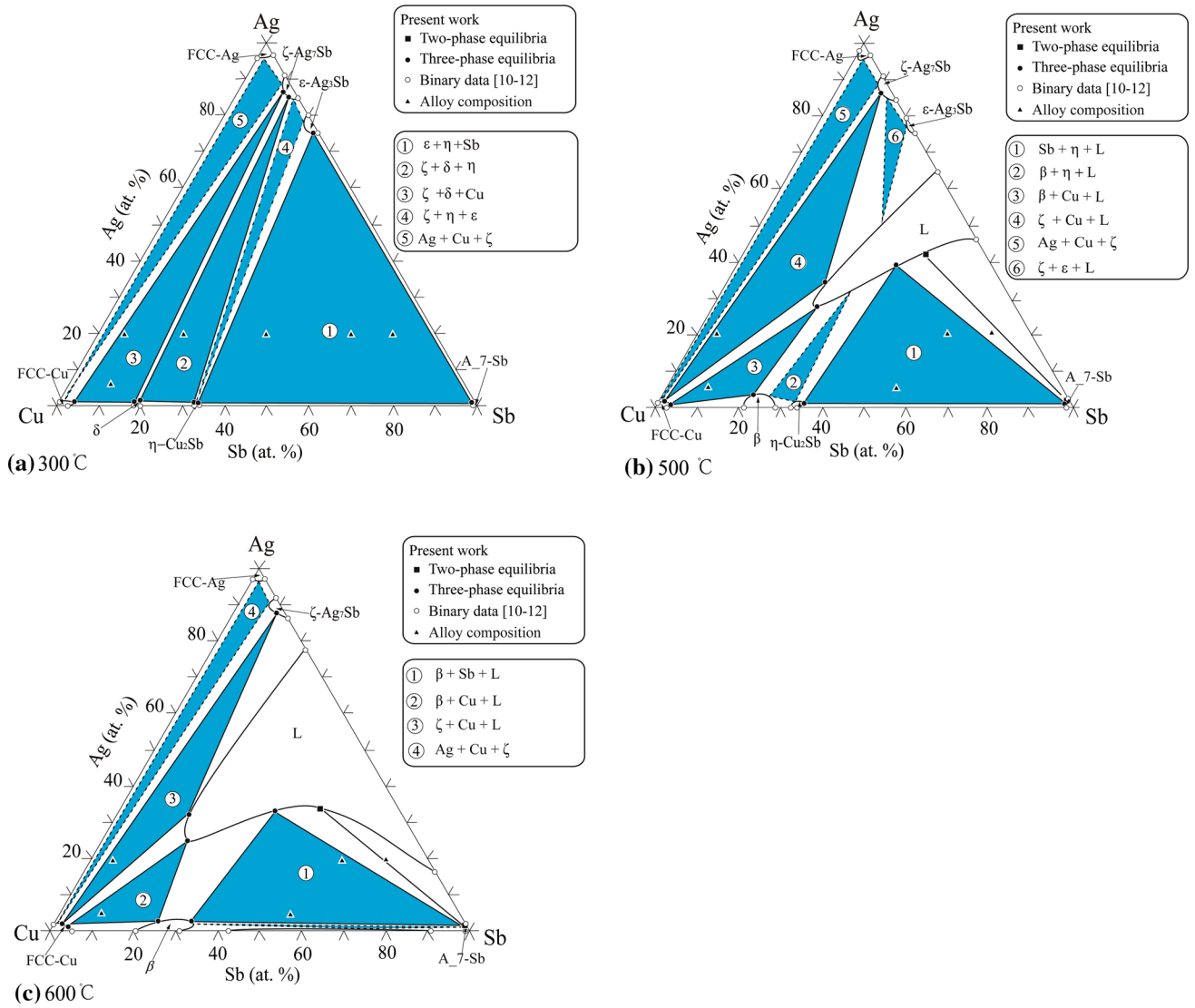


**Fig. 4** Experimentally determined isothermal sections of the Ag-Cu-Sb system: (a) 300 °C, (b) 500 °C, (c) 600 °C

**Acknowledgments**

This work was supported by the National Natural Science Foundation of China (Nos. 51031003 and 51171159), the Ministry of Education Foundation of China (No. 20120121130004). National Key Basic Research Program of China (973 program) (No. 2012CB825700) is also acknowledged.

**References**

1. D. Suraski and K. Seelig, The Current Status of Lead-Free Solder Alloys, *IEEE Trans. Electron. Packag. Manuf.*, 2001, **24**(4), p 244-248
2. K.W. Moon, W. Boettinger, U. Kattner, F. Biancaniello, and C. Handwerker, Experimental and Thermodynamic Assessment of Sn-Ag-Cu Solder Alloys, *J. Electron. Mater.*, 2000, **29**(10), p 1122-1136
3. C.S. Oh, J.H. Shim, B.J. Lee et al., A Thermodynamic Study on the Ag-Sb-Sn System, *J. Alloy Compd.*, 1996, **238**(1), p 155-166
4. S. Chen, A. Zi, W. Gierlotka et al., Phase Equilibria of Sn-Sb-Cu System, *Mater. Chem. Phys.*, 2012, **132**(2), p 703-715
5. X.J. Liu, M. Kinaka, Y. Takaku, I. Ohnuma, R. Kainuma, and K. Ishida, Experimental Investigation and Thermodynamic Calculation of Phase Equilibria in the Sn-Au-Ni System, *J. Electron. Mater.*, 2005, **34**(5), p 670-679
6. X.J. Liu, R. Kainuma, I. Ohnuma, K. Ishida, and K. Oikawa, The Use of Phase Diagrams and Thermodynamic Databases for Electronic Materials, *JOM*, 2003, **55**(12), p 53-59
7. F. Gao, C.P. Wang, X.J. Liu, Y. Takaku, I. Ohnuma, and K. Ishida, Experimental Investigation and Thermodynamic Calculation in the Ag-Bi-Ni and Cu-Bi-Ni Systems, *J. Electron. Mater.*, 2009, **24**(08), p 2644-2653
8. C.P. Wang, F. Huang, Y. Lu, S.Y. Yang, M. Yang, and X.J. Liu, Experimental Investigation and Thermodynamic Calculation of the Phase Equilibria in the Cu-Ni-Sb Ternary System, *J. Electron. Mater.*, 2013, **42**(10), p 2961-2974

9. C.P. Wang, L.H. Zhao, Y. Lu, D. Wang, Y.H. Guo, S.Y. Yang, and X.J. Liu, Experimental Investigation and Thermodynamic Calculation of the Phase Equilibria in the Bi-Cu-Zn Ternary System, *J. Phase Equilib. Diffus.*, 2014, **35**(5), p 530-543
10. X.J. Liu, F. Gao, C.P. Wang, and K. Ishida, Thermodynamic Assessments of the Ag-Ni Binary and Ag-Cu-Ni Ternary Systems, *J. Electron. Mater.*, 2008, **37**(2), p 210-217
11. W. Gierlotka, Y.C. Huang, and S.W. Chen, Phase Equilibria of Sn-Sb-Ag Ternary System: Calculation, *Metall. Mater. Trans. A*, 2008, **39**(13), p 3199-3209
12. X.J. Liu, C.P. Wang, I. Ohnuma, R. Kainuma, and K. Ishida, Thermodynamic Assessment of the Phase Diagrams of the Cu-Sb and Sb-Zn Systems, *J. Phase Equilib. Diffus.*, 2000, **21**(5), p 432-442
13. Y.W. Yen and S.W. Chen, Phase Equilibria of the Ag-Sn-Cu Ternary System, *J. Mater. Res.*, 2004, **19**(8), p 2298-2305
14. S. Nagakura, S. Toyama, and S. Oketani, Lattice Parameter and Structure of Silver-Copper Alloys Rapidly Quenched from Liquid State, *Acta Metall.*, 1966, **14**(1), p 73-75
15. H.T. Luo and S.W. Chen, Phase Equilibria of the Ternary Ag-Cu-Ni System and the Interfacial Reactions in the Ag-Cu/Ni Couples, *J. Mater. Sci.*, 1996, **31**(19), p 5059-5067
16. E. Zoro, C. Servant, and B. Legendre, Thermodynamic Modeling of the Ag-Au-Sb Ternary System, *J. Phase Equilib. Diffus.*, 2007, **28**(3), p 250-257
17. B. Bokstein and A. Smirnov, Grain Boundary Segregation in Cu-Sb Alloys, *Mater. Lett.*, 2003, **57**(29), p 4501-4504
18. W. Gierlotka and D. Jendrzeczyk-Handzlik, Thermodynamic Description of the Cu-Sb Binary System, *J. Alloy Compd.*, 2009, **484**(1), p 172-176
19. E. Hayer, K. Komarek, and R. Castanet, A Thermodynamic Investigation of the Copper-Antimony System, *Z. Metallkd.*, 1977, **68**(10), p 688-696
20. C. Lee, C.Y. Lin, and Y.W. Yen, The 260 C Phase Equilibria of the Sn-Sb-Cu Ternary System and Interfacial Reactions at the Sn-Sb/Cu Joints, *Intermetallics*, 2007, **15**(8), p 1027-1037
21. X.P. Su, N.Y. Tang, and J.M. Toguri, 450°C Isothermal Section of the Fe-Zn-Si Ternary Phase Diagram, *Can. Metall. Q.*, 2001, **40**(3), p 377-384